

# MESH SENSOR FOR HIGH TEMPERATURE HIGH PRESSURE APPLICATIONS

**John Kickhofel\*** and **Horst-Michael Prasser**

Laboratory of Nuclear Energy Systems

ETH Zurich

Sonneggstrasse 3, 8057 Zurich

Switzerland

kickhofel@lke.mavt.ethz.ch; prasser@lke.mavt.ethz.ch

**Karthick Selvam and Eckart Laurien**

Institute of Nuclear Technology and Energy Systems

University of Stuttgart

Pfaffenwaldring 31, 70569 Stuttgart

Germany

karthick.selvam@ike.uni-stuttgart.de; eckart.laurien@ike.uni-stuttgart.de

**Hermann Huber**

Materials Testing Institute

University of Stuttgart

Pfaffenwaldring 32d, 70569 Stuttgart

Germany

hermann.huber@mpa.uni-stuttgart.de

## ABSTRACT

State-of-the-art turbulence models are expected to accurately predict flow behavior in a wide range of geometries and flow conditions for a wide range of fluid properties. The validation and improvement of these models relies on accurate time resolved experimental measurements of scalar and vector flow variables. One such measurement technique for obtaining a high density of flow data with high time resolution is electrode mesh tomography in the form of wire mesh sensors. Extensive studies on single and multiphase flows have been successfully carried out with mesh sensor technology in the past 15 years, often focused on flows directly related to nuclear power generation. Nearly all of these experiments have taken place at low temperatures (< 100°C) and pressures.

A new mesh sensor construction has been designed for operation in high temperature and pressure steam and water environments similar to those found in commercial light water reactors. The sensor package is compatible with standard flanged steel pipelines by implementing a novel electrode design and sealing methodology, while relying on the traditional mesh sensor electronics which processes current signals from the receiver wires simultaneously at up to 10 kHz. Furthermore, the design allows for a scaling of the sensor not only in terms of electrode pitch but the possibility to include a third sensor layer or a second in-line mesh sensor for velocity measurements based on cross-correlations. We describe in detail a prototype sensor of 16 x 16 electrodes compatible with DN80 PN100 flanges and exhibit sensor commissioning data from mixing experiments the University of Stuttgart high temperature high pressure fluid-structure interaction T-junction facility. Specifically, flow patterns in the main pipe of the T-junction due to upstream flow of cold branch line fluid are measured using the new mesh sensor.

## KEYWORDS

Mesh sensors, T-junction, Thermal Fatigue, Turbulent Mixing, Thermal Stratification

## 1. INTRODUCTION

Measurements of high temperature high pressure single and multiphase flows are valuable sources of information for both theoreticians and practitioners in the field of nuclear engineering. A great deal of research in the nuclear thermal hydraulic domain is generated from low temperature or fully adiabatic tests in atmospheric pressure environments. The transition from data gathered from such tests to a clear understanding of thermal hydraulic or fluid dynamic behavior at the working conditions of a nuclear power plant (NPP), so-called scaling, is nontrivial. Some of the challenge of scaling could be avoided by more experimental data of a higher density in space and time from existing test facilities which are constructed to operate nearer to or at the temperature and pressure conditions found in NPPs.

Wire mesh sensors have seen successful implementation in experimental studies of single and multiphase flows for nearly 20 years. Based on technology developed by Prasser (1998), the sensors measure the electrical conductivity (EC) of a medium as analog current detected in a multiplexed-manner where each transmitter electrode is sequentially delivered a square-wave voltage pulse during which all receiver electrodes are sampled in parallel. Cross-talk between neighboring receivers or transmitters is suppressed by means of low-impedance drivers and inputs for the transmitters and receivers, respectively. The measurement technology is typically applied in, but not limited to, closed conduits such as flow channels or pipelines where the EC may be measured throughout the cross section of the duct with a typical resolution, determined by the pitch of the electrodes, of 1 to 5 mm.

It is the intention of this paper to introduce a mesh sensor package design platform which is relatively uncomplicated and whose sealing methodology and materials provide for potential expansion or modification of the internal sensor structure relative to the current state-of-the-art [1]. Previous state of the art is detailed in publications by Prasser (2008), Dudlik (2008) and Pietruske (2007), all originating from the Forschungs Zentrum Rossendorf (FZR now HZDR) in Germany [2-4]. These publications demonstrate two distinct high temperature mesh sensor designs, of which both have relied on ‘high temperature’ epoxies, rated to 180°C, to ensure an effective pressure barrier.

The rod-electrode type design utilized large electrodes, by mesh sensor standards, of 5 mm in height and 1.5 mm width (with a leaf-shape cross section to reduce pressure drop) which were fixed on one end and allowed to thermally expand freely, along their axis, on the other. This design, first implemented at FZR, went on to be manifest in successful measurement campaigns at the PMK-2 test facility (in DN80) at the KFKI-AEKI in Hungary and the PPP facility (in DN50 and DN100) of UMSICHT in Germany as a part of the OECD/NEA Primary Coolant Loop Test Facility (PKL-2) Project [5].<sup>i</sup> These sensor ranged in size from a DN100 version with 16 transmitter and 16 receiver electrodes rated for 180°C at 7 MPa, to a DN80 12 x 12 electrodes version rated for 250°C also at 7 MPa. The latter sensor were designed with integrated water cooling, outside of the pressure barrier, to ensure the integrity of the epoxy sealing.

A spring-based high temperature wire mesh sensor design, described by Pietruske (2007), benefits from thin 0.25 mm diameter stainless steel wire electrodes while the overall construction is admittedly “extremely complicated” [3]. Thermal expansion and contraction is managed by a system of compression or tensile springs in concert with ceramic insulation pearls requiring extensive machining of the sensor flanges. Two sensor constructions were manufactured, assembled, and tested in steam-water and air-water multiphase flows at the TOPFLOW facility at FZR, both with 3 mm wire pitch and 2 mm between the two layers. The smaller sensor was of 16 x 16 electrodes for a DN50 conduit, the larger, comprised of 64 x 64 electrodes was installed in a DN200 pipeline. The maximum temperature and pressure ratings for both sensors was declared to be 7 MPa and the corresponding saturation temperature of 286°C. The larger of the two sensors prohibited the installation of all 12 bolts in the

---

<sup>i</sup> In the framework of the EURATOM project WAHALoads.

DN200 flanges, only 8 could be utilized, which meant a special licensing procedure had to be carried out with the authority responsible for pressurized equipment.

This paper is divided into two halves. The first, Section 2, focuses on the new high temperature wire mesh sensor design and materials while the second half, Section 3, demonstrates some results from proof of concept testing of the new sensor at the fluid structure interaction T-junction facility at the University of Stuttgart in Germany.

## 2. SENSOR DESIGN

The sensor package is notable for a separation of the pressure barrier construction from the mesh sensor itself. The result is a package design which allows for a variety of potential sensor designs to be incorporated. For example, two mesh sensors or a three layer sensor could be incorporated to measure flow velocities based on the cross-correlation technique of Prasser (2013) [6]. Two steel housing flanges comprise the bulk of the sensor package, they act to provide a cavity within the pressure barrier of the facility, assured by the three gaskets, which is large enough such that a mesh sensor and associated wiring may be mounted. The two flanges, so-called primary and lid flanges, surround and secure the mesh sensor sandwich, see Figure 1. During operation, the entire cavity around the sensor sandwich as well as the feedthrough conduits are filled with the working fluid and are within the pressure barrier.

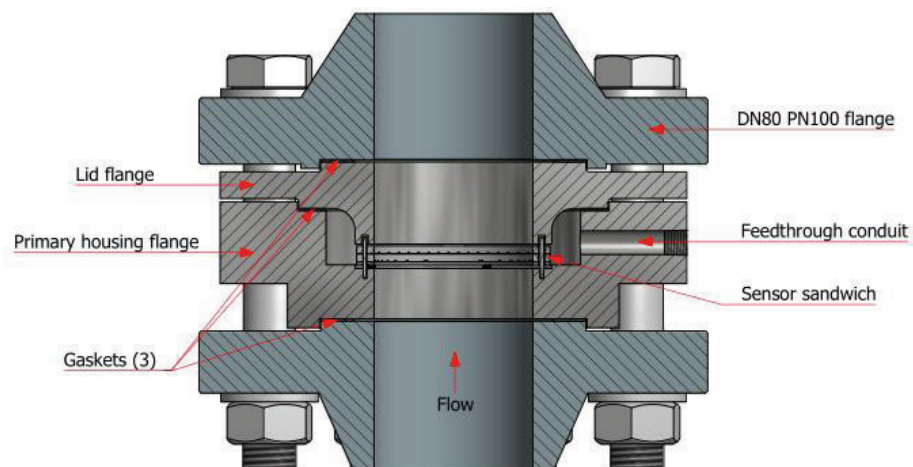


**Figure 1. CAD drawing of sensor package installed in DN80 PN100 flanged pipeline of inner diameter 71.8mm.**

### 2.1 Sensor package

The housing flanges allow for the transport of the mesh sensor as a pre-assembled unit which need only be installed on-site between two un-modified flanges in the pipeline. The design maintains the ability to execute the usual sealing strategy (e.g. the appropriate number of bolts) for the flanged pipeline in which the sensor is installed, in this case that for DN80 PN100 flanges. The primary housing flange accepts the sensor, centering pins and compression springs. The lid flange acts as an adapter to seal the sensor inside of the primary housing flange while also providing the appropriate connection, e.g. tongue-and-groove, to the pipeline flange. In the primary housing flange two feedthrough conduits are machined perpendicular to the flow direction (and to each other) through which transmission wires, spliced to the mesh sensor electrodes, are fed via Swagelok® pressure hoses to their respective Conax Technology® sealing glands, one for the transmitter signals and one for the receiver electrodes, where they finally pass through the final pressure barrier. Outside of the pressure barrier connection is made to a SUBD 25-type screw terminal which is linked via shielded cables to the data acquisition unit. The purpose of the pressure hoses is to provide greater physical separation between the sealing glands, which

have a temperature rating of 260°C, and the heat source, be it the fluid itself or external heating pads. The sealing glands are rated for up to 22 MPa.

A consequence of the additional space in the conduit provided by the housing flanges is that the gasket which ensures the sealing between the two is of larger diameter than those found in the pipeline itself. The gasket between the housing flanges is of inner/outer diameter Ø116/140 mm such that the sealing area is similar to that of the standard Ø90/120 mm gaskets found in DN80 PN100. The result is non-negligible stress in the form of torsion acting on both housing flanges by the pipeline flanges they are connected to. CATIA V5 finite element simulations have been performed based on a 300°C ambient with 100 MPa internal pressure and conservative forces on the gasket surfaces estimated based on 200 Nm bolt torque. Results show maximum von-Misses stresses of 290 MPa in the lid flange and 350 MPa in the primary housing flange. These values are well above the  $R_{p0.2}$  offset yield strength of standard stainless steels at 300°C. Therefore, the stainless martensitic chromium-nickel-molybdenum steel 1.4418 was chosen for the sensor package housing flanges. With a yield strength of 580 MPa at 300°C, high Cr content, and the addition of Molybdenum, 1.4418 is an ideal candidate for the requirements of the sensor package in high temperature water/steam environments [7].

## 2.2 Sensor Sandwich

The sensor itself is comprised of three ceramic plates which are held in place by two 1.5 mm diameter centering pins and compressed together by four small springs. The ceramic plates are made of Photoveel II, a proprietary-blend machinable nitride ceramic manufactured by Ferrotec Europe GmbH, which has a rated thermal shock resistance of 600 K making it suitable for environments where large temperature gradients are expected such as in stratified flows or quenching scenarios [8]. Two 3 mm thick ceramic plates act to hold and position the receiver and transmitter electrodes, respectively, by means of 0.6 mm wide 0.6 mm deep grooves, 16 per plate. The result is separation of approximately 2.4 mm between the electrode layers. A third, 1.5 mm thick ceramic plate, completes the stack, ensuring electrical isolation of the uppermost layer of electrodes from the lid flange.

The 16 receivers and 16 transmitter electrodes are positioned with a pitch of 4.49 mm such that 208 crossing points (between a transmitter,  $t$ , and receiver,  $r$ ) lie within the 71.8 mm diameter main pipe at the Stuttgart T-junction. A schematic and photo of the sensor is shown in Figure 2. The electrodes are 316L stainless steel capillaries of mean OD 0.57 mm and mean ID 0.31 mm. Splicing between the electrodes and transmission wires is achieved by means of 0.90 mm OD, 0.67 mm ID 316L stainless steel crimps. The transmission wires are PTFE insulated stranded wire with nineteen 0.10 mm OD silver coated copper conductors.

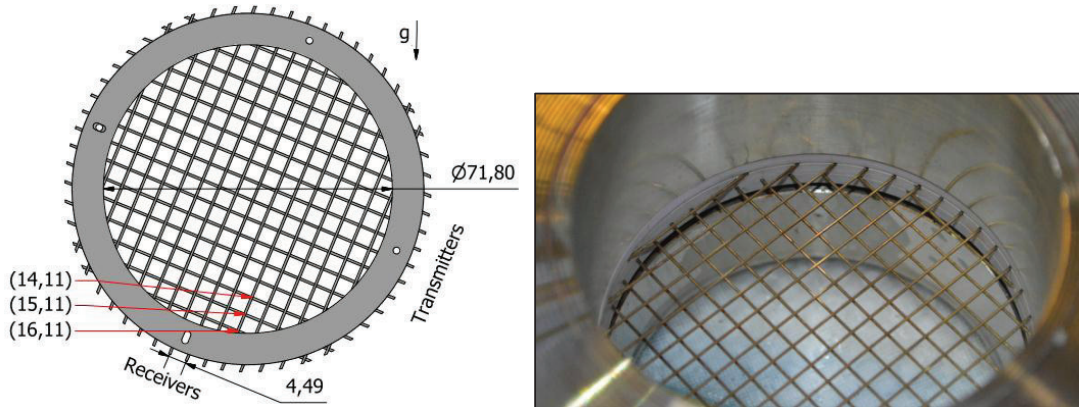


**Figure 2. Schematic (left) of the 16 by 16 electrode mesh sensor with 4.49 mm pitch and 71.8 mm diameter. Gravity vector,  $g$ , is according to the installation orientation at the T-junction facility. Three crossing points ( $t,r$ ) near the bottom of the pipe are referred to later in the Results section. Photograph (right) of the mesh sensor sandwich installed between the housing flanges.**

### 3. PROOF OF CONCEPT

At the University of Stuttgart in Germany, the Institute of Nuclear Technology and Energy Systems (IKE) and the Materials Testing Institute (MPA) have, since 2011, operated a T-junction facility (Fluid–Structure Interaction Setup Stuttgart) for the study of fluid structure interaction in the case of large fluid temperature differences. The facility incorporates reactor-grade materials (such as the forged austenitic stainless steel T-junction with reduced carbon content in accordance with the German KTA 3201.1) [9] and can reach reactor-like conditions with  $\Delta T$  approaching 240 K. The facility, shown schematically in Figure 3 has been utilized for proof-of-concept testing of the sensor. In brief, a  $D_m = 71.8$  mm ID main pipe carrying hot water at a constant mass flow rate of 0.4 kg/s (turbulent flow) encounters a perpendicular, horizontal branch pipe of 38.9 mm ID with room temperature water flowing at a rate of 0.1 kg/s (transition flow). Downstream the flow is then split according to the mass flow rate ratio and recycled back to the T-junction. The edge of the junction is sharp. Flow conditions at the T-junction are such that at low  $\Delta T$  ( $=T_m - T_b$ ) a wall-jet type flow pattern is manifest downstream of the T-junction at these flow rates. At higher  $\Delta T$  the cold branch line flow quickly sinks to the bottom of the mixing pipe downstream of the T-junction and only weakly mixes with the hotter main flow. More information about the flow behavior at the facility is described in the work of Kuschewski (NWLED-IF experiments), Klören (LES simulations), and, most recently, Selvam (LES simulations) [10-15]. Understanding of cross-flow mixing behavior in T-junctions at high  $\Delta T$  suffers due to a lack of published experimental data, with most facilities studying cross flow mixing at  $\Delta T < 60$  K.

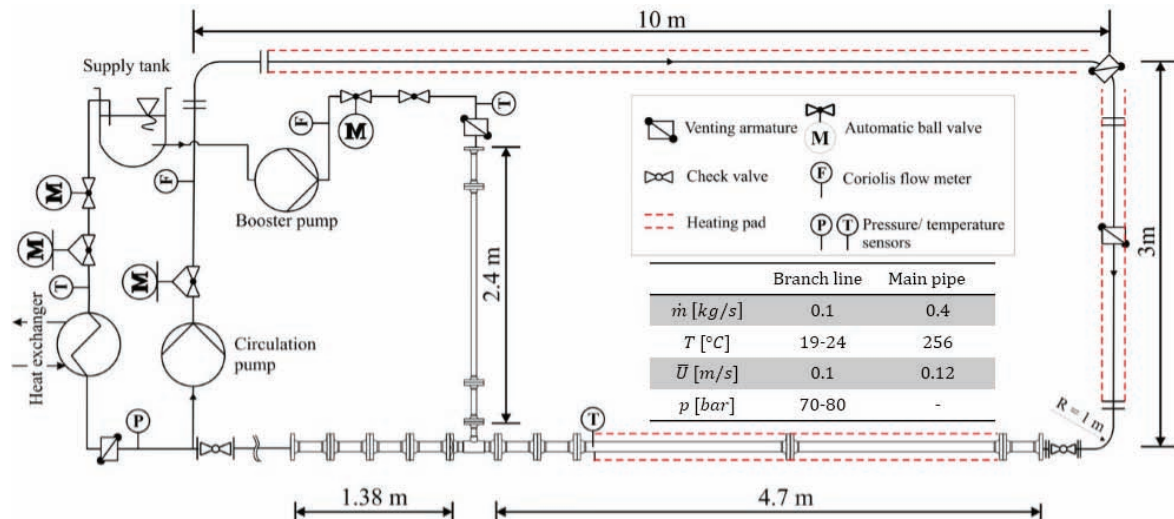


**Figure 3. Piping and instrumentation diagram of the University of Stuttgart T-junction facility adapted from Kuschewski (2013).[11]**

The phenomena of upstream flow of the cold branch fluid in the main pipe experienced at high  $\Delta T$  has been described by few publications. The authors are aware only of the LES simulations by Klören (2013) with regards to the Stuttgart T-junction, and, separately, experiments by Chen (2012, 2014) at the EXTREM vertical branch T-junction facility at the NTHU Taiwan at  $\Delta T = 90$  K [15-18].<sup>ii</sup> Klören

<sup>ii</sup> Here we exclude discussing in-passing mentions of the minute and highly transient upstream or ‘reverse flow,’ sometimes noticed in low  $\Delta T$  mixing studies, e.g. by Tanaka (2010). That phenomena is categorically different from the lengthy upstream flow found at high  $\Delta T$  discussed in this paper.

finds that for  $\Delta T = 150$  K in the Stuttgart geometry, upstream flow proceeds  $> 3 D_m$  in the main pipe and  $> 25 D_m$  for  $\Delta T = 260$  K at the same flow rate conditions measured by the mesh sensor, while LES simulations by Selvam (2015) anticipate upstream flow to around  $0.5 D_m$  at  $\Delta T = 123$  K with a higher main mass flow rate of  $0.6 \text{ kg/s}$ .

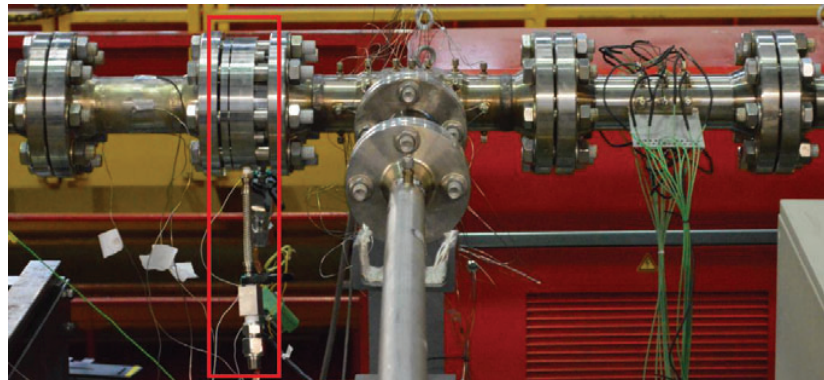


**Figure 4.** Mesh sensor package (highlighted in red box) installed upstream of the T-junction.

The mesh sensor was installed at the nearest possible position upstream of the T-junction such that the measurement plane of the mesh sensor is located at  $-3.48 D_m$ , see Figure 4. Flow in the main pipe of the T-junction facility was heated continuously from room temperature to its highest operating temperature of  $256^\circ\text{C}$  at  $7 \text{ MPa}$ . The hot flow is measured  $1015 \text{ mm}$  upstream of the T-junction in the center of the main pipe by a thermocouple (XTM3). Room temperature water was continuously flowing through the branch line during heating, i.e. mixing at the T-junction never ceased during the experiment, the temperature of which was recorded by a thermocouple (XTM4) in the center of the branch line flow  $2940 \text{ mm}$  upstream of the T-junction. This process consumed approximately eight hours during which wire mesh sensor measurements were triggered every  $253$  seconds for a duration of  $180$  seconds, the  $73$  seconds between measurements being required for downloading and saving the data. The measurement frequency of every crossing point was  $10 \text{ kHz}$ . The temperature history in the main pipe and branch line, recorded once a minute, is shown in Figure 5.

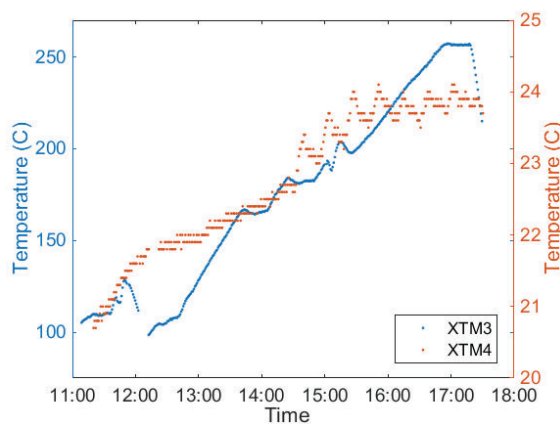


**Figure 5.** Plot of main pipe (XTM3, blue, left y-axis) and branch line (XTM4, red, right y-axis) flow temperatures during the experiment.

### 3.1 Calibration methodology

The sensor electronics are identical to those driving traditional mesh sensor technology; the measurement principle is, furthermore, also the same. The sensor measures the EC of a small volume of fluid between each crossing point. Typically single phase mixing experiments, such as studies of turbulent mixing at T-junctions, would utilize a salt tracer to differentiate the main flow from the branch flow and therefore capture the mixing process. The addition of a tracer was not possible at the T-junction facility and therefore the measurements rely on the varying EC of water with temperature. The ion product,  $K_w = [H^+][OH^-]$  (also referred to as the dissociation constant), of pure water has been measured by Marshall (1981) over a wide range of temperatures and pressures and subsequently accepted by the International Association for the Properties of Water and Steam (IAPWS).<sup>[19]</sup> Figure 6 (left) shows the EC of pure water vs. temperature at 7 MPa based on the correlation and coefficients of Marshall.

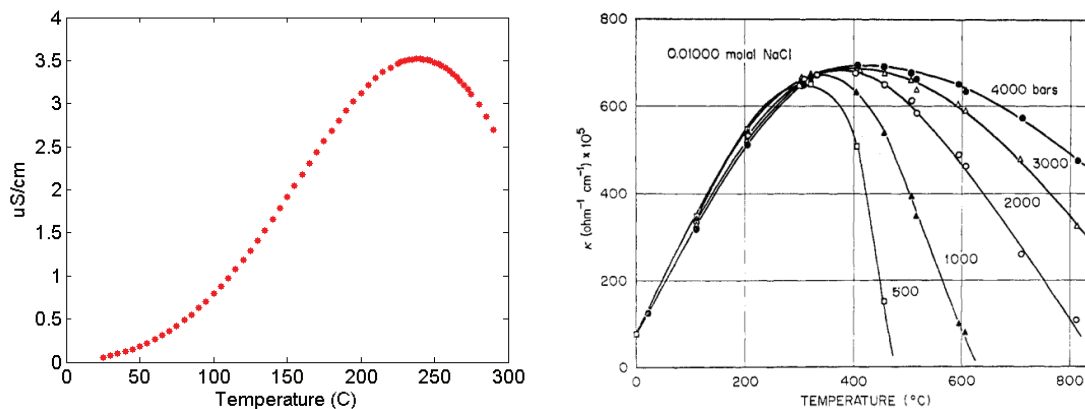


**Figure 6. EC vs. temperature (left) according to the correlation of Marshall (1981) for pure water, and EC vs. temperature (right) from experiments with NaCl solutions at high pressure from Quist (1967).<sup>[19, 20]</sup>**

Truly pure water, however, does not exist in an engineering context. Measurements by a handheld meter at the T-junction facility found the circulated water to have EC of 7-9  $\mu\text{S}/\text{cm}$ , which results in a different shape of the ion product vs. temperature curve. It has been shown, for electrolyte solutions such as NaCl, for example, that EC is nearly linear to 200°C over a wide range of pressures, see Figure 6 (right).<sup>[20]</sup> The mobility of ions in the water are the dominating contribution, compared to the self-dissociation of  $\text{H}_2\text{O}$ , to the EC as a function of temperature especially at elevated temperatures in the range of interest.<sup>iii</sup> The peak in EC is the result of ionic association counterbalancing the ionic mobility as the density of water continues to decrease with temperature. The nonlinearity of EC as a function of temperature, seen especially below 100 C, is lost with an increase in impurities. Therefore, a linear behavior of the EC of the water over a range between approximately 60 and 200°C has been assumed.

The calibration of the mesh sensor at the Stuttgart T-junction is performed using the raw data collected from the full day of heating and cooling the facility. For the calibration of each crossing point, a single reference thermocouple was chosen. The reference thermocouple, XTM3, described earlier, lies in the center of the flow 765 mm upstream of the mesh sensor. It would be incorrect to assume that the temperature at XTM3 is equal to the temperature across the whole of the mesh sensor plane. A number of factors are at play; firstly, there is no heating of the flow between XTM3 and the mesh sensor plane; some heat losses and mixing can be expected. Secondly, and more importantly, at a Reynolds number of 54,000 (at 200°C) in the main pipe the flow is not sufficiently turbulent such that a flat temperature profile is achieved in the pipe cross section. A top-to-bottom temperature gradient in the main pipe is

<sup>iii</sup> The sharp decrease in viscosity of water vs temperature as it is heated above room temperature is the reason for increased ionic mobility.

expected to exceed 10-15 K at high water temperatures based on thermocouple measurements at the facility. Therefore, a least squares regression was performed to best estimate the reference temperature at each mesh sensor crossing point  $T_{t,r}$ , as a function of reference thermocouple temperature  $T_r$ , and time  $t$ .

A least squares regression seeks the planar fitting of 3D points of the form  $(x, y, T_r(t_{max}))$ . The plane  $T_r + A + By + Cx$  describes the distribution of temperature in the pipe cross section at the location of the mesh sensor which is known to exhibit a gradient from top to bottom at high temperatures.<sup>iv</sup> We seek the minimum of the function,

$$R^2 = \sum_i^{16} \sum_j^{16} (T_r(t_{max,ij}) + A + By_{ij} + Cx_{ij} - T_{ij}(t_{max,ij}))^2, \quad (1)$$

$$\frac{\partial(R^2)}{\partial A} = 0, \frac{\partial(R^2)}{\partial B} = 0, \frac{\partial(R^2)}{\partial C} = 0, \quad (2)$$

where  $T_{t,r}(t_{max,t,r})$  is defined for all  $t,r$  crossing points as 240°C: the temperature corresponding to the maximum signal, and therefore maximum EC, at each crossing point. The reference thermocouple reading  $T_r$ , at the time of maximum signal at crossing point  $t,r$ ,  $t_{max,t,r}$ , varies. In this way a function for the estimated temperature at each crossing point at any given time,  $T_{t,r} = T_r(t) + A + By_{t,r} + Cx_{t,r}$ , may be generated assuming a planar temperature profile in the cross section at 240°C. A further step is taken to scale the coefficients  $B$  and  $C$  with main flow temperature, assuming that the temperature profile in the main pipe must be flat at room temperature (20°C),

$$B'(t) = B \left( -\frac{20}{220} + \frac{1}{220} T_r(t) \right) = B \left( \frac{T_r(t)-20}{220} \right), \quad (3)$$

and similarly for  $C'(t)$ . An example of the relationship between the corrected reference temperature,  $T_{t,r}$ , and the mesh sensor signal  $\theta$ , is shown in Figure 7. Visible is the peak in the EC of the water at 240°C. The region in which the crossing points are calibrated is where the signal shows linear dependence to the temperature. A linear fit is made in this region for each crossing point which becomes function which converts the raw measured signals to temperatures.

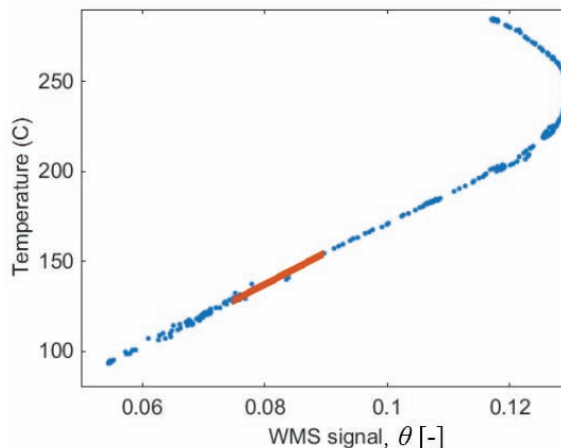


**Figure 7. Plot of raw mesh sensor signal  $\theta$  vs. estimated temperature at a crossing point near the top of the pipe. The function which describes the linear fit, shown in red, is that which converts signal values to temperature at this crossing point for any given measurement dataset.**

---

<sup>iv</sup> The x-component is included to account for the possibility of upstream swirl influencing the temperature profile along this axis.

Due to the design of the T-junction facility it is not possible avoid mixing at the T-junction, the branch flow cannot be eliminated. Therefore, the presence of cold upstream flow at the mesh sensor precludes the generation of complete calibration data for the crossing points of the sensor at the bottom of the pipe. We therefore rely on the linear behavior of the EC of the fluid versus temperature in calibrating these crossing points for temperatures that we could otherwise not verify being experienced at those locations (estimated as temperatures above 140°C).

#### 4. RESULTS

Upstream of the T-junction the measurements at and beyond the onset of upstream flow are of greatest interest. Prior to the presence of upstream flow at the sensor a mild average temperature gradient in the hot flow is detected with negligible temperature fluctuations. The mesh sensor detected the onset of upstream flow as the  $\Delta T$  between the main and branch flows was increasing past 143 K. A number of crossing points at the bottom of the pipe detect a sudden drop in temperature for which the cold branch line water is responsible. Rather than detecting a slow, downward ramping of the temperature, the temperature at the bottom of the pipe plummets rapidly. Figure 8 shows the temperature at three consecutive, neighboring crossing points found different distances from the wall at the bottom of the pipe. The first sign up cold flow reaching the sensor at  $-3.48 D_m$  is a dip of up to 20°C at the crossing point nearest to the wall. The temperature then rebounds back to that of the bulk flow (150°C+) within two seconds before moments later ( $< 0.5$  s) plummeting below 100°C and never again reaching temperatures higher than 125°C. Part of that initial thermal shock includes a portion in which the fluid changed temperature from 140°C to 100°C at a rate of approximately -130°C/s. Near the wall, once the cold flow arrives the temperature fluctuations are significant at lower crossing points:  $T_{RMS}(16,11) = 6.3$  K and  $T_{RMS}(15,11) = 8.4$  K in the first 10 seconds after the onset of upstream flow. The fluctuations, while remaining sizable, are greatly reduced in magnitude some 10's of seconds later, between 30 and 40 s after the onset of upstream flow,  $T_{RMS}(16,11) = 3.1$  K and  $T_{RMS}(15,11) = 5.2$  K. Over the course of the 180 s measurement, which captures the onset of upstream flow within the first 10 seconds<sup>v</sup>, it would appear from the results that the area of cold fluid seen by the sensor is growing, while the bulk main flow temperature as measured by XTM3 has increased marginally, by 1.2°C.

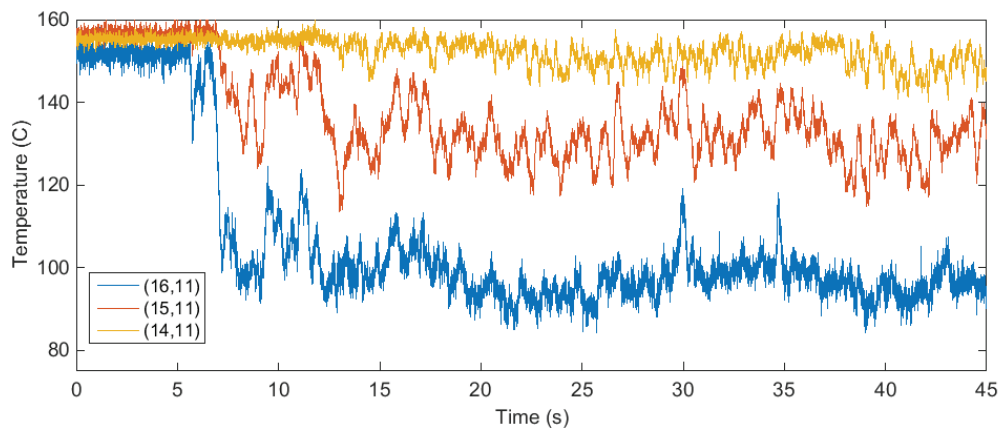


**Figure 8. Temperature at three mesh sensor crossing points (location indicated in Figure 2) at the bottom of the main pipe during the onset of upstream flow reaching the sensor location (-3.48  $D_m$ ). Measurements were recorded at 2000 Hz and smoothed with a 10 point moving average.**

<sup>v</sup> It is impossible to rule out the possibility that upstream flow reached the sensor prior to this in the 73 seconds of downtime between this measurement which appears to have captured the onset of the flow and the previous measurement which shows no indication of temperature changes at the bottom of the pipe.

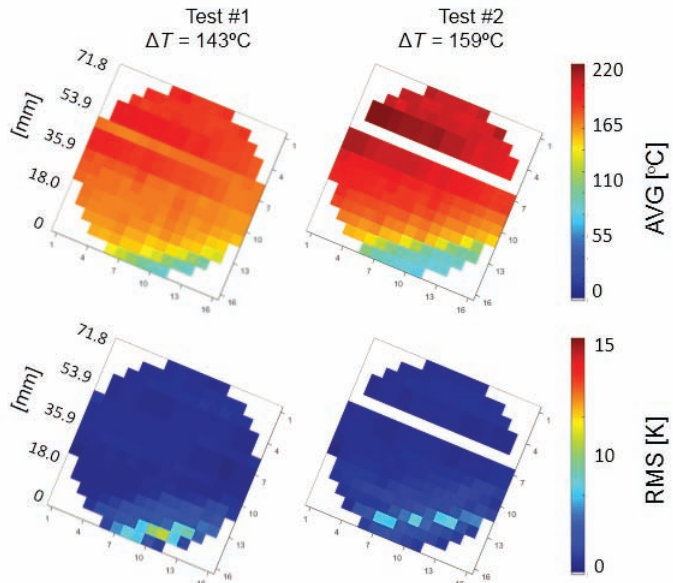


**Figure 9.** Plot of time-averaged temperature and RMS of the temperature looking away from the T-junction at  $-3.48 D_m$  at two mixing conditions, (a)  $165.5^\circ\text{C}$  main pipe and  $22.5^\circ\text{C}$  branch line ( $\Delta T \approx 143 \text{ K}$ ) and (b)  $181.5^\circ\text{C}$  main pipe and  $23.2^\circ\text{C}$  branch line ( $\Delta T \approx 158 \text{ K}$ ).

Heating of the facility was stabilized twice for approximately 10 minutes, once at  $164.5\text{-}166.5^\circ\text{C}$  in the main pipe ( $\Delta T \approx 143 \text{ K}$ ) and another at  $181\text{-}182^\circ\text{C}$  ( $\Delta T \approx 158 \text{ K}$ ). Both mean and RMS values at these conditions are shown in Figure 9, transmitter number 6 is left blank or draws from only a portion of the measurement due to a noisy signal which resulted in limited usable data. At  $\Delta T \approx 143 \text{ K}$  the mesh sensor measures a small amount of upstream flow at the very bottom of the pipe with temperature of approximately  $100^\circ\text{C}$ . Neighboring crossing points sees a mean temperature increase of over 30 degrees. The highest temperature fluctuations are found in the thin layer between the cold upstream flow and the hot main flow. The remainder of the cross section shows negligible temperature fluctuations. With higher temperature difference ( $\Delta T \approx 158 \text{ K}$ ), and therefore density difference, at the T-junction the amount of upstream flow in the pipe cross section is increased and the temperature gradient between the zone of upstream flow and the hot flow is considerably larger. The RMS of the temperature, however, is decreased compared to the lower  $\Delta T$  case, which can be interpreted as a more stable stratification.

The power spectral density (PSD) of the temperature signal at a given crossing point has been computed as follows,

$$PSD(\omega) = \left[ \int_0^{t_{end}} \theta(t) e^{-i\omega t} dt \right]^2, \quad (4-1)$$

where  $\theta(t)$  is the signal from each crossing point and  $t_{end}$  is the duration of the raw signal which is comprised of three 180 measurements. The full length signal is cut in to  $K$ -segments of duration  $t_k$ , with 0% overlap and without windowing,

$$\theta(t) = \sum_1^K \theta_k(t). \quad (4-2)$$

The PSD is then computed for each segment and all  $K$  spectra are then averaged to create the final, ensemble averaged spectrum,

$$PSD_k(\omega) = \left[ \int_0^{t_k} \theta_k(t) e^{-i\omega t} dt \right]^2, \quad (4-3)$$

$$\langle PSD_k(\omega) \rangle = \frac{1}{K} \sum_1^K PSD_k(\omega). \quad (4-4)$$

Figure 10 shows plots of the 4-times ( $K=4$ ) ensemble averaged temperature signal for both flow conditions at three crossing points near the bottom of the main pipe.

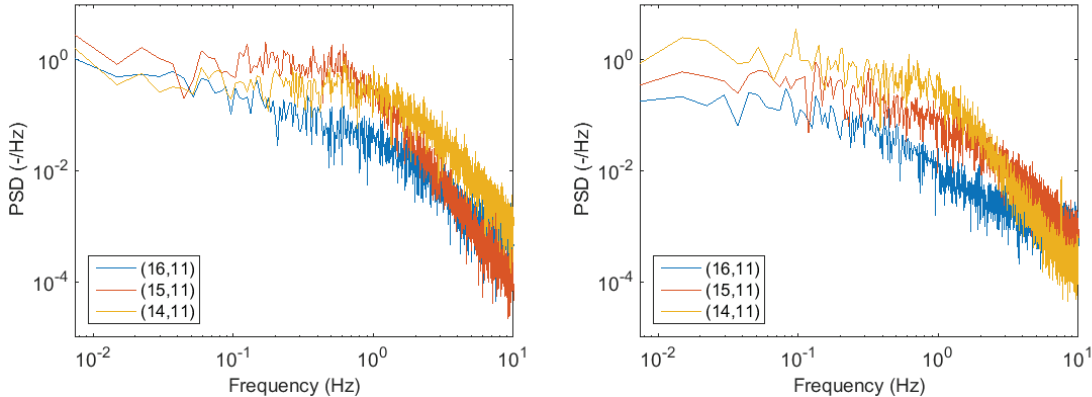


**Figure 10. PSD at three crossing points near the bottom of the main pipe at  $\Delta T \approx 143$  K (left) and  $\Delta T \approx 158$  K (right).**

At  $\Delta T \approx 143$  K the highest RMS is measured at (15,11), the PSD at this position shows a plateau at frequencies below 0.7 Hz without strong evidence of a preferred mixing frequency. A larger portion of the RMS of the temperature arises from low frequencies in the mixing layer (15,11) than above (14,11) or below (16,11) it. In the case of a larger temperature gradient, at  $\Delta T \approx 158$  K, the crossing point (14,11) lies within the mixing zone between the cold upstream flow and the hot main flow. The mixing spectrum at this crossing point also exhibits a plateau at lower frequencies with a peak at 0.1 Hz. Considering the materials and geometries of interest, 0.1 to 1 Hz is typically cited as the range of interest related to thermal fatigue [21].

## CONCLUSIONS

A novel mesh sensor package for high temperature and high pressure has been design, constructed and tested. The design benefits from a pressure barrier solution which separates the need for the sensor construction or electrodes themselves to have a pressure sealing capability. The result is a sensor design which can be easily incorporated into flanged pipelines and has the potential incorporate large volumes of electrodes and thermocouples. The sensor has been tested in single phase flows at temperatures of at least 256°C at 7MPa pressure in the presence of large thermal gradients. The design in theory is capable of measuring single and multiphase flows at both BWR and PWR conditions, up to 350C and 220 bar by using enamel coated conductors, rather than PTFE or PEEK, and sealing glands with higher pressure ratings.

Proof-of-concept measurements validated the feasibility of the sensor design and furthermore resulted in measurements of the unique T-junction mixing issue of upstream flow in the main pipe encountered only at high density differences between the mixing water, the result of high  $\Delta T$ . The results indicate high thermal gradients in the bulk flow and near-wall. Furthermore, the onset of backflow at the location of the mesh sensor was not measured as a slow, steady decrease in temperature at the bottom of the pipeline but rather a rapid drop in temperature more akin to quenching, raising the concern of high cycle

thermal fatigue should this thermal shock phenomena take on a more transient nature, in the case of varying main flow velocities due to global instabilities, for example.

Besides the proof of the sensor technology at high thermodynamic parameters, the experiments show that temperatures can be measured via the temperature dependent electrical conductivity of water. It is on one hand admittedly less accurate than more direct temperature sensors, but has on the other hand the advantage of covering an entire cross-section in a comparatively cheap way and of providing temperature histories with a time resolution that is much higher than in case of thermocouples or other sensors with considerable thermal inertia. In the present work, we took benefit from this feature by using the raw signals to obtain RMS values of the temperature in the mixing process. Spectral information is planned to be extracted as well.

## REFERENCES

1. J. Kickhofel and H.-M. Prasser, "Grid Sensor Package," European Patent Application EP14198142, (2014).
2. H.-M. Prasser, G. Ézsöl, G. Baranyai and T. Sühnel, "Spontaneous Water Hammers In A Steam Line In Case Of Cold Water Ingress," *Multiphase Science and Technology* **20** (3-4), pp. 265-289 (2008).
3. H. Pietruske and H.-M. Prasser, "Wire-mesh sensors for high-resolving two-phase flow studies at high pressures and temperatures," *Flow Meas Instrum* **18** (2), pp. 87-94 (2007).
4. A. Dudlik, H.-M. Prasser, A. Apostolidis and A. Bergant, "Water hammer induced by fast acting valves—experimental studies at Pilot Plant Pipework," *Multiphase Science and Technology* **20** (3-4), pp. 239–263 (2008).
5. OECD/NEA, <https://www.oecd-nea.org/jointproj/pkl-2.html>, Accessed: Febrary 27 2015.
6. H.-M. Prasser, "Generalized Cross-correlation Technique For The Measurement Of Time-dependent Velocities," presented at the The 15th International Topical Meeting on Nuclear Reactor Thermal - Hydraulics, NURETH-15, Pisa, Italy, (2013).
7. *Key to Steel - Stahlschlüssel*. (Verlag Stahlschlüssel Wegst GmbH, Marbach, Germany, 2013).
8. F. E. GmbH, <https://ceramics.ferrotec.com/products/ceramics/materials/machinable/nitride/>, Accessed: February 3.
9. D. K. A. KTA, "KTA 3201.1 Komponenten des Primärkreises von Leichtwasserreaktoren - Teil 1: Werkstoffe und Erzeugnisformen," 1998-06.
10. M. Kuschewski, R. Kulenovic and E. Laurien, in *14th International Topical Meeting on Nuclear Reactor Thermalhydraulics (NURETH-14)* (Toronto, Ontario, Canada, 2011).
11. M. Kuschewski, R. Kulenovic and E. Laurien, "Experimental setup for the investigation of fluid-structure interactions in a T-junction," *Nucl Eng Des* **264**, pp. 223-230 (2013).
12. D. Kloeren, M. Kuschewski and E. Laurien, "Large-Eddy Simulations of Stratified Flows in Pipe Configurations Influenced by a Weld Seam," presented at the CFD for Nuclear Reactor Safety Applications (CFD4NRS-4) Workshop, Daejeon, Korea, (2012).
13. P. K. Selvam, R. Kulenovic and E. Laurien, "Large eddy simulation on thermal mixing of fluids in a T-junction with conjugate heat transfer," *Nucl Eng Des* **284**, pp. 238-246 (2015).
14. K. Selvam, R. Kulenovic and E. Laurien, in *International Congress on Advances in Nuclear Power Plants (ICAPP)* (Charlotte, USA, 2014).
15. D. Klören and E. Laurien, "Large-Eddy Simulations of Stratified and Non-stratified T-junction Mixing Flows," *High Performance Computing in Science and Engineering '12: Transactions of the High Performance Computing Center, Stuttgart (HLRS)*, pp. 311-324 (2013).
16. M.-S. Chen, H.-E. Hsieh, Y.-M. Ferng and B.-S. Pei, "Experimental observations of thermal mixing characteristics in T-junction piping," *Nucl Eng Des* **276**, pp. 107-114 (2014).
17. M.-S. Chen, Y.-M. Ferng, H.-E. Hsieh and B.-S. Pei, in *ANS Annual Meeting* (Chicago, Illinois, USA, 2012).
18. M. Tanaka, H. Ohshima and H. Monji, "Thermal Mixing in T-Junction Piping System Related to High-Cycle Thermal Fatigue in Structure," *Journal of Nuclear Science and Technology* **47** (9), pp. 790–801 (2010).

19. W. L. Marshall and E. U. Franck, "Ion product of water substance, 0–1000°C, 1–10,000 bars New International Formulation and its background," *Journal of Physical and Chemical Reference Data* **10** (2), pp. 295 (1981).
20. A. S. Quist and W. L. Marshall, "Electrical Conductances of Aqueous Sodium Chloride Solutions from 0 to 800 Degrees and at Pressures to 4000 Bars," *Journal of Physical Chemistry* **72** (2), pp. 684-703 (1967).
21. L.-W. Hu, J. Lee, P. Saha and M. S. Kazimi, in *Third International Conference on Fatigue of Reactor Components* (Seville, Spain, 2004).